ISSN: 2639-0108

Research Article

Advances in Theoretical & Computational Physics

Invisible Bubbles with Liquid Wall from Dark Plasma of the Sun§

Sapogin V.G[1] and Sapogin K.V[2*]

[1]2 App. 3 Frunze Street, Taganrog, Rostov Region, 347922, Russia

[2]Department of Astronomy, University of Minnesota, 116 Church Street SE, Minneapolis, MN 55455, USA

[*]Corresponding Author
Sapogin K.V., Department of Astronomy, University of Minnesota, 116 Church Street SE, Minneapolis, MN 55455, USA.

Submitted: 2024, Sep 20; **Accepted:** 2024, Oct 24; **Published:** 2024, Nov 12

Citation: Sapogin, V. G., Sapogin, K. V. (2024). Invisible Bubbles with Liquid Wall from Dark Plasma of the Sun§. *Adv Theo Comp Phy, 7*(4), 01-18.

Abstract

The article presents fragments of canonical physics of mass particles' collective interaction. Equations of self-consistent statics of mass particles and their solutions are given. The integral of "living forces" in plane symmetry is found. It allows to validate the field confinement of matter by a self-consistent field. A pair of forces of field origin, holding the layer in a static equilibrium state, is found - the compression force and the expansion force. The distribution of physical parameters in a flat layer is investigated. The thickness of layer is determined. It coincides with doubled spatial scale.

An approximate solution to the problem of matter distribution in a hollow cold cluster with uniform temperature is found in spherical field traps of the first kind. The approximate solution is verified by numerical simulation. An exact solution is found for potential distribution in a field trap of the second kind. Estimates show that mass spectra of hollow neutron clusters with temperatures from 10^{11} to 10^{12} K can be identified with masses of objects observed in centers of galaxies.

A hypothesis has been put forward about the existence of invisible gas bubbles of small radii and large masses with low temperatures. Flying out from dark plasma of the Sun, filled balls, due to expansion and cooling activity of gas, turn into thin-walled bubbles with liquid wall. The expansion process transfers them to the class of dark matter. Collisions with invisible bubbles can be responsible for depressurization of spacecraft, for inelastic impacts on station windows, and even for unsuccessful landings of space modules on the Moon. Processing the trajectory measurements of lunar modules' unsuccessful landing will confirm or refute the hypothesis of their collisions with invisible bubbles.

Keywords: Invisible Bubbles, Liquid Wall, Solar Dark Plasma, Field Confinement

1. Introduction

The solution of equilibrium problems for a substance of mass particles in isolated gas sphere has been proposed by theoretical physics since the end of nineteenth century. The first works were published by Lane and Emden. Two classes of ordinary differential equations of the second order were constructed. The first class described filled gas spheres in polytropic states with non-uniform temperature. The second class - the Emden *E*-equation, which describes a gas accumulation with a uniform temperature [1]. It was assumed that the static state of mass particles' equilibrium is maintained by the action of two forces: the attractive force and the repulsive force of gas pressure.

Exact solutions, describing the state of equilibrium of gas sphere, completely filled with particles, were found for various polytropic indices. All solutions had a maximum density at the center of sphere and also satisfied the boundary conditions $y(0)=1, y'(0)=0$ at the center of sphere. The gravitational force compressed the substance to the center of sphere and counteracted the force of gas pressure. Chandrasekhar related the results of obtained solutions to the theory of stars and got the observed values of physical parameters on the Sun for polytropic index n=3 [2]. It is necessary to note an interesting feature of obtained solution. The initial equations were written for gas sphere of particles, and the calculations determined the parameters of solar plasma, which was in the liquid phase.

For gas with spherical symmetry Emden did not find a solution that would give the maximum density in the center of sphere. As shown in the work, the reason could be that the equation had an unexpected class of solutions for hollow sphere with no matter in

the center of it.

Independently of Emden's research, apparently even without any knowledge about them, in 1948 Frenkel introduced a similar method for calculating fields for mass particles' gas with constant temperature and called the macroscopic static fields, holding the matter, self-consistent [3]. Indeed, the analysis of the Frenkel equations in vector form indicates that the Bernoulli force coincides with the pressure gradient of collective field and the system of particles is held in limited region of space by this field. The equations describe the field confinement of matter. A new understanding of the physics of matter confinement allows us to find solutions in the Emden-Frenkel equations for gas balls with a cavity and for thin-walled bubbles.

If Emden wrote down the equation for the density of a gas ball, then Frenkel constructed them for the potential of the gravitational field created by the cluster collective. Solving the problem of the distribution of matter in a spherical cluster, he has come to the unexpected conclusion that the exact solution he found for concentration of matter leads to results devoid of physical meaning.

The work shows that the correct physical interpretation of solutions, existing in spherical symmetry, can only be obtained after a detailed analysis of the conditions and causes of the equilibrium of matter with the collective field in plane symmetry. This path leads to the appearance of the integral of "living forces" in the system and allows us to construct a fragment of the canonical physics of collective interaction of heated and cold clusters of mass particles in states with any density. The discovered exact solutions and their new interpretation transfer the equations of theoretical astrophysics of Emden-Chandrasekhar-Frenkel to a higher level of significance - the level of canonical physics.

2. Basic Equations of the Problem

Using Frenkel's approach [3], we write down three-dimensional equations of equilibrium of matter in a collective field, which in modern notations of vector analysis have the form

$$\rho\vec{g} + \vec{f} = 0\,; \tag{2.1}$$

$$div\vec{g} = -4\pi\gamma\rho\,; \tag{2.2}$$

$$\vec{g} = -grad(\varphi)\,; \tag{2.3}$$

$$p = \rho kT/m\,; \tag{2.4}$$

$$\vec{f} = -grad(p)\,. \tag{2.5}$$

Here ρ – is the mass density in an elementary volume, $\vec{g}$ – is the intensity of the macroscopic collective gravitational field, p – is the gas-kinetic pressure inside the system, T – is the absolute temperature of the system, φ – is the potential of the self-consistent field, γ – is the gravitational constant, m – is the mass of the gravitating particle, k – is the Boltzmann constant, f – is the Bernoulli force.

The first equation of the system is the equilibrium condition of the elementary volume of the system of gravitating particles. The second is the differential form of Newton's law (Poisson's equation), which allows one to calculate static fields of smeared masses with negative divergence. Equation (2.3) gives the relationship between the potential and the intensity of the gravitational field. And (2.4) is the equation of state with a uniform temperature. Equation (2.5) is the definition of the static Bernoulli force. Note that the relationship between the intensity and the potential (2.3) has not used by Emden in his study.

Let us show that the complete system of equations (2.1-2.5) reflects the collective interaction between mass particles, in which the reverse action of the field on the particles, generating this field, is manifested.

3. Equation of Self-Consistent Statics of Mass Particles

Substituting (2.5) and (2.3) into (2.1), we obtain

$$\rho grad(\varphi) + grad(p) = 0\,. \tag{3.1}$$

Taking into account the equation of state (2.4) and the homogeneity of temperature, we bring (3.1) to the form

$$grad\left(\frac{m\varphi}{kT} + \ln\rho\right) = 0\,. \tag{3.2}$$

From (3.2) it is clear that any equilibrium of gravitating particles with a uniform temperature is characterized by a scalar integral

$$\frac{m\varphi}{kT}+\ln\rho=\frac{m\varphi_0}{kT}+\ln\rho_0=const, \tag{3.3}$$

where ρ_0 and φ_0 are constants.
From (3.3) follows the exponential Boltzmann distribution function

$$\rho=\rho_0 exp\left[-m(\varphi-\varphi_0)/kT\right]. \tag{3.4}$$

It indicates the inverse effect of the field on the density of distributed particles. Where the potential of the collective field is higher, the density of particles is lower.

Substituting (3.4) into (2.2), we express everything through φ and collapse the system of equations (2.1) - (2.5) into one equation

$$\Delta\varphi=4\pi\gamma\rho_0 exp\left[-m(\varphi-\varphi_0)/kT\right]. \tag{3.5}$$

Equation (3.5) is three-dimensional field analogue of an equation in the form of the Emden *E*-equation, which describes the distribution of macroscopic potential in systems of particles with uniform temperature that are in static equilibrium with a self-consistent field. The positivity of the right-hand side of (3.5) indicates that the system consists of a collective of particles that create a field with negative divergence. Equation (3.5) is given by Frenkel in [3].

4. The Integral of "Living Forces" of the Emden-Frenkel E-Equation in Plane Symmetry

Equation (3.5) for plane symmetry has the form

$$\varphi''=4\pi\gamma\rho_0 exp\left[-m(\varphi-\varphi_0)/kT\right], \tag{4.1}$$

where the primes mean differentiation with respect to the *x* coordinate. Written in dimensionless variables, $y=(\varphi-\varphi_0)/\varphi_*$, $\varphi_*=2kT/m$, $\xi=x/l$, where $l=\sqrt{\varphi_*/4\pi\gamma\rho_0}$ – is the spatial scale of a plane system. Equation (4.1) has the form $y''=f(y)$

$$\frac{d^2y}{d\xi^2}=e^{-2y}.$$

It allows for a reduction in order and leads to the integral of "living forces" [4]

$$\frac{(y')^2}{2}+U(y)=const,\quad U(y)=-\int f(y)dy=e^{-2y}/2.$$

For the initial variables, it corresponds to the total pressure of system, first found in [5]:

$$\frac{(\varphi')^2}{8\pi\gamma}+p(\varphi)=P=H(\varphi',\varphi)=const, \tag{4.2}$$

where $p(\varphi)=p_0 exp\left[-m(\varphi-\varphi_0)/kT\right]$ – gas-kinetic pressure of heated particles of system in the plane with potential φ, and $p_0=n_0kT=\rho_0\varphi_*/2$ – pressure of particles of system in the plane.

The total pressure *P* of system in (4.2) consists of two terms: the first term is the pressure of self-consistent field of system, and the second is the pressure of particles. The first integral (4.2) coincides with the Hamiltonian function $H(\varphi',\varphi)$, in which the canonically conjugate quantities are $\varphi'/4\pi\gamma$, generalized momentum $\varphi'/4\pi\gamma$ and generalized coordinate φ. The role of generalized time is played by the coordinate *x*.

Equality (4.2) is satisfied in the absence of any external static gravitational fields considered with respect to the self-consistent field of the system. The class of even functions of potential of the self-consistent field and their derivatives is always established like this. In any plane taken inside the system, the sum of pressures of the field and particles of the system remains unchanged.

Conservation law (4.2) also means that in any plane of the system under consideration, the gradients of pressures of self-consistent field and particles of the system are equal to each other, but have different directions. The volume density of the Bernoulli force (hereinafter the Bernoulli force) (2.5) is the force, expanding the layer. It is opposite to the particle pressure gradient. In the problem

it receives a new mathematical definition: the Bernoulli force coincides in magnitude and direction with the pressure gradient of the collective field compensates for the compression forces and ensures a class of equilibria of particles with the field that they create themselves.

Substituting the mass density from equation (2.2) into (2.1), we obtain the relationship between the Bernoulli force and the pressure gradient of self-consistent field $\vec{G}$

$$\vec{f} = -\rho\vec{g} = \frac{\vec{g}}{4\pi\gamma} div\vec{g} = \vec{G}, \tag{4.3}$$

which, together with (2.5), gives the physical condition for holding an elementary volume of matter by self-consistent field

$$\vec{G} + grad(p) = 0. \tag{4.4}$$

If the field of the system under study is one-component and flat one, $g = [g_x(x)\,0,0]$, then equality (4.4) takes the form

$$G_x + \frac{dp}{dx} = \frac{g_x}{4\pi\gamma}\frac{dg_x}{dx} + \frac{dp}{dx} = \frac{d}{dx}\left(\frac{g_x^2}{8\pi\gamma} + p\right) = 0$$

and leads to the integral of total pressure (4.2).

Equality (4.4) indicates a previously unknown property of self-consistent gravitational field to hold an inhomogeneous system of particles in a limited region of space by static forces of field origin. It follows from this that the system of collective interaction of particles is in static equilibrium with a self-consistent field if the sum of pressure gradients of the field and particles is equal to zero in any elementary volume of the system.

5. Distribution of Physical Parameters in a Flat Layer

Integrating (4.2) under the condition that the value φ_0 corresponds to the extremum of the potential function (it's realized when $P = p_0$), and placing this extremum at the origin x=0, we obtain the law of potential distribution along the length of the system

$$\varphi = \varphi_0 + \varphi_* log\left[cosh\left(\frac{x}{l}\right)\right], \tag{5.1}$$

where

$$l = \sqrt{kT/(2\pi\gamma m\rho_0)} = \frac{1}{m}\sqrt{\frac{kT}{2\pi\gamma n_0}} \tag{5.2}$$

is spatial scale of the system, $d = 2l$ - scale of wall thickness, and $\varphi_* = 2kT/m$ – scale of potential.

As can be seen from (5.1), the distribution of the potential along the length of system has the form of potential wells with infinite walls that by turn have a minimum with the value φ_0 in the plane x=0.
The projection of self-consistent field strength is distributed along the length of system according to the law:

$$g_x = -\varphi' = -g_0 tanh(x/l), \tag{5.3}$$

where $g_0 = \varphi_*/l = 2kT/ml$ – scale of the strength. As can be seen from (5.3), the field strength of system vanishes in the plane x=0, and at $x/l \to \pm\infty$ $g_x \to \mp g_0$. The system has no sharp boundaries, since the density, concentration and pressure of particles have a distribution in form of a soliton with a maximum at the bottom of the well

$$\frac{\rho}{\rho_0} = \frac{n}{n_0} = \frac{p}{p_0} = cosh^{-2}(x/l). \tag{5.4}$$

As can be seen from (5.3) and (5.4), the field squeezes the particles into the minimum of potential energy of the system. Its intensity remains uniform in those places where the substance is absent. The distribution of field pressure along the length of the system follows from (5.3):

$$D = (\varphi')^2 / 8\pi\gamma = D_0 \tanh^2(x/l), \tag{5.5}$$

where $D_0 = p_0 = g_0^2/(8\pi\gamma)$ – is the scale of field pressure.

From relations (5.5) and (5.4) it is clear that the sum of pressures of particles and the field of system in any plane of the interaction space remains constant and equal to the total pressure of system $P = p_0$, which is the integral of system. The result of differentiation (5.5) shows that the gradient of field pressure in any plane of system is opposite to the gradient of particle pressure following from (5.4), and is equal to it in absolute value:

$$dD/dx = -dp/dx = f_0 \tanh(x/l)/\cosh^2(x/l), \tag{5.6}$$

Where $f_0 = 2p_0/l$ is the scale of volume density of holding forces. It is proportional to the value of $\sim \rho_0^{3/2} T^{1/2}$. The forces holding a cluster of mass particles should be called the Emden-Frenkel forces, which are the discoverers of basic equation.

The directions of gradients allow us to determine the directions of volume forces, holding the system in equilibrium. The compression force of the layer is directed toward the plane x=0 and coincides with the direction of the vector $\vec{g}$. The Bernoulli forces that expand the system are created by the pressure gradient of self-consistent field (4.3), which compensates for the action of particle pressure gradient.

Mathematical equalities (2.5) and (4.3) indicate the dual role of self-consistent field that forms the trap configuration. On the one hand, the field creates a pressure gradient in the substance, co-directed with its intensity vector (2.3). And on the other hand, the same field creates a static force (4.3), which compensates for the emerging gradient.

Field boundary conditions adequate to the problem can be formulated as follows: the system must have a surface on which the pressure of self-consistent field vanishes and the potential - is minimal. In the flat case, this surface lies in the x=0 plane. In the spherical case, as shown in the next section, the formulated boundary conditions can be realized only at a finite distance from the center of system.

6. Spherical Field Traps of the First Kind

Let us write equation (3.5) in spherical symmetry for the radial dependence of the potential:

$$\varphi'' + 2\varphi'/r = 4\pi\gamma m n_0 \exp\left[-m(\varphi-\varphi_0)/kT\right], \tag{6.1}$$

where $n_0 = \rho_0/m$ – the value of concentration of particles of the system on the sphere $\varphi = \varphi_0$ and the primes mean differentiation with respect to r.

Passing in (6.1) to the function $y(x) = -(\varphi-\varphi_0)/\varphi_*$ with respect to the variable x=r/R, where R is the radius of the sphere on which field boundary conditions are satisfied, we bring (6.1) to the form

$$xy'' + 2y' + \alpha^2 x \exp(2y) = 0, \tag{6.2}$$

where

$$\alpha^2 = \frac{2\pi\gamma m^2 n_0 R^2}{kT} = \frac{T_*}{T} = \frac{R^2}{l^2} \tag{6.3}$$

- the state parameter of the system, and

$$T_* = \frac{2\pi\gamma m^2 n_0 R^2}{k} \tag{6.4}$$

- its temperature scale (the primes mean differentiation with respect to x). The state parameter of the system α allows for a double interpretation. On the one hand, it allows us to compare the temperature of the system with its scale, and, on the other hand, to compare the radius of the sphere on which boundary conditions are satisfied with the spatial scale of system *l* (5.2).

Equation (6.2) belongs to the class of equations of type *E* - the Emden-Frenkel equation [1-3], which describes non-uniform distributions of matter in a gas ball with a uniform temperature, and is its field analogue.

7. Approximate Solutions of the Problem

We will seek approximate solutions (6.2) for boundary conditions $y(1)=0,\ y'(1)=0,$ that assume the existence of a zero-pressure field sphere in the cluster. These solutions describe the distribution of physical parameters of system in field traps of the first kind. Passing to a new function

$$y(x)=\eta(\xi)-\xi,\quad y'=\frac{d\xi}{dx}\left(\frac{d\eta}{d\xi}-1\right),\ \text{where}\ \xi=\ln x,$$

we obtain the equation

$$\frac{d^2\eta}{d\xi^2}+\frac{d\eta}{d\xi}=1-\alpha^2\exp(2\eta) \tag{6.5}$$

with boundary conditions $\xi=0$, $\eta(0)=0$, $\frac{d\eta}{d\xi}(0)=1,$ which allows a reduction in order by introducing a new function

$$p(\eta)=\frac{d\eta}{d\xi};\quad \frac{d^2\eta}{d\xi^2}=p\frac{dp}{d\eta}.$$

The first-order equation

$$p\frac{dp}{d\eta}+p=1-\alpha^2\exp(2\eta) \tag{6.6}$$

has boundary conditions $\eta=0, p(0)=1$. It cannot be integrated in elementary functions. In [6], a numerical solution of equation (6.6) was carried out for a family of integral curves passing through the boundary condition point. The solution indicates the existence of an Emden singular point at $\eta=\eta_s>0$, in which $p\to 0$, and $dp/d\eta\to-\infty$. In Fig. 1 shows four integral curves in coordinates $p=p(\eta)$. Curve 1 is constructed for α=0.5; curve 2 – for α=1.0; curve 3 – for α=1.5; curve 4 – for α=2.0.

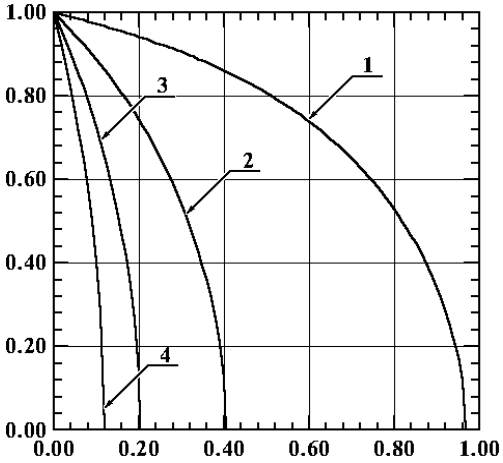

Figure 1: Integral Curves p=p(η)

As can be seen from Fig. 1, the position of the Emden singular point $\eta=\eta_s$ depends on the value of α^2. For small α^2 it is located far from the origin $\eta=0$. For values $\alpha^2>>1$ the singular point approaches the origin from the right. This allows us to find an approximate solution (6.6) when the condition $\alpha^2>>1$ is met.

Let us solve (6.6) with respect to the derivative:

$$\frac{dp}{d\eta}=\frac{1-\alpha^2 exp(2\eta)}{p}-1. \tag{6.7}$$

If the condition

$$\alpha^2 exp(2\eta)/p >> 1/p-1 \tag{6.8}$$

is satisfied, equation (6.7) can be shortened, reduced to the form

$$\frac{dp}{d\eta}=-\frac{\alpha^2 exp(2\eta)}{p} \tag{6.9}$$

and integrated in elementary functions

$$p=\sqrt{1-\alpha^2\left[exp(2\eta)-1\right]}. \tag{6.10}$$

Let us determine the values of the parameter α for which approximation (6.8) is satisfied. To do this, let us represent (6.8) in the form:

$$\alpha^2 >> (1-p)exp(-2\eta)=f(\eta).$$

The largest value of the function $f(\eta)$ on the right-hand side of the inequality corresponds to the value of the Emden singular point $\eta=\eta_s$. Then approximation (6.8) is satisfied under the condition

$$\frac{1}{\alpha^2+1}<<1, \tag{6.11}$$

which is satisfactory even for α =3 and is improved with increasing α.

Returning to the function $\varphi(r)$ in (6.10), we obtain a family of curves describing the distribution of the potential along the length of system in the case where the temperature of system is less than the scale (state of cold cluster):

$$\frac{\varphi}{\varphi_*}=\frac{\varphi_0}{\varphi_*}+log\left[\frac{\alpha r}{R\sqrt{1+\alpha^2}}cosh(A)\right], \tag{6.12}$$

where

$$A=Ar\,cosh\left(\frac{\sqrt{1+\alpha^2}}{\alpha}\right)-\sqrt{1+\alpha^2}\,log\left(\frac{r}{R}\right),$$

α and φ_0 are the distribution parameters.

As can be seen from (6.12), the radial distributions of the potential have the form of potential wells with infinite walls that have a minimum $\varphi=\varphi_0$ on the sphere of zero field pressure.

Expression (6.12) allows us to obtain in analytical form the main gravistatic and kinetic characteristics of cluster for the case $\alpha^2>>1$. The projection of the r-th component of the self-consistent field strength is found from (6.12) and has the form

$$\frac{g_r}{g_*} = \frac{RB}{r}, \tag{6.13}$$

where $g_* = \frac{2kT}{mR}$ – is new scale of the strength; $B = \sqrt{1+\alpha^2}\,tanh(A) - 1$.

Distribution of density, concentration and pressure of particles in the cluster:

$$\frac{\rho}{\rho_0} = \frac{p}{p_0} = \frac{n}{n_0} = \left[\frac{\alpha r}{R\sqrt{1+\alpha^2}}\cosh(A)\right]^{-2}. \tag{6.14}$$

The pressure of self-consistent field inside the cluster changes according to the law:

$$D = \frac{g_r^2}{8\pi\gamma} = D_* \frac{R^2 B^2}{r^2}, \tag{6.15}$$

where $D_* = p_0 / \alpha^2 = g_*^2 /(8\pi\gamma)$ – is new scale of field pressure.

The projection of the radial component of the compensating Bernoulli force has the form

$$f_r = -\frac{dp}{dr} = -\frac{f_* R^3 (1+\alpha^2) B}{\alpha^2 r^3 \cosh^2(A)}, \tag{6.16}$$

where $f_* = 2p_0 / R$ – is new scale of pressure gradient.

The radial projection of field pressure gradient is distributed according to the law

$$G_r = \frac{g_r}{4\pi\gamma r^2}\left[\frac{d}{dr}\left(r^2 g_r\right)\right] = \frac{4D}{r} + \frac{dD}{dr} = \frac{f_* R^3 B}{\alpha^2 r^3}\left(B - \frac{1+\alpha^2}{\cosh^2 A}\right). \tag{6.17}$$

The condition of confinement of the substance by self-consistent field (4.4) takes the form

$$G_r + \frac{dp}{dr} = \frac{f_* R^3 B^2}{\alpha^2 r^3} = 0 \tag{6.18}$$

As can be seen from (6.12) – (6.16), the sphere of zero field pressure divides entire interaction space of the cluster into two regions: internal $0 < r/R < 1$ and external $r/R \geq 1$. In the internal region, the strength of self-consistent field coincides with the direction of radius vector. In it, with increasing *r*, the potential decreases, and the pressure and concentration of particles increase. In the external region, the direction of field strength vector is opposite to the direction of radius vector. In it, with increasing *r*, the potential increases, and the pressure and concentration of particles decrease. The system has no sharp boundaries. Since the field squeezes the substance into minimum of potential energy, a cavity is formed inside the cold cluster in which the substance is practically absent.

To analyze the behavior of the system near the bottom of potential well, we introduce the axis ξ, directed along the radius vector, with the origin at point *r*=*R*: $r = R + \xi$. Expanding (6.12) in a Taylor series by small parameter with accuracy to quadratic terms, we obtain dependences of physical parameters similar to flat symmetry:

$$\varphi(\xi) \approx \varphi_0 + \varphi_* \alpha^2 \xi^2 /(2R^2); \qquad g_\xi \approx -g_* \alpha^2 \xi / R;$$

$$D(\xi) \approx D_* \alpha^4 \xi^2 / R^2; \qquad p(\xi) \approx p_0\left(1 - \alpha^2 \xi^2 / R^2\right);$$

$$P = D(\xi) + p(\xi) = p_0 = const; \qquad \frac{d}{d\xi}\left[D(\xi) + p(\xi)\right] = 0.$$

The confinement condition in the form of (6.18) is well satisfied in thin quasi-flat layers located at the bottom of potential well ($B^2 \approx 0$). At a singular point $r \to \infty$ of system, the confinement condition is also satisfied since (6.18) tends to zero according to the law $\sim r^{-3}$:

$$G_r + \frac{dp}{dr} \approx \frac{f_* R^3}{\alpha^2 r^3}\left(1+\sqrt{1+\alpha^2}\right)^2 .$$

At another singular point of system, the confinement condition is poorly satisfied, since at $r \to 0_+$

$$G_r + \frac{dp}{dr} \approx \frac{f_* R^3}{\alpha^2 r^3}\left(\sqrt{1+\alpha^2}-1\right)^2 \to \infty \ .$$

The reason for this may be presence of cavity in which the substance is absent. In [7] it is shown that obtained approximate solution (6.12) turns out to be exact for any α in cylindrical symmetry. It describes the distribution of mass particles in long heated tubes, cold hollow tubes and tubes with thin wall.

An estimate of the number of cluster particles held by a self-consistent field is obtained after integrating the expression

$$N_1 = \int_0^\infty n(r) 4\pi r^2 dr = \frac{3n_0 V(1+\alpha^2)}{\alpha^2 R}\int_0^\infty dr / cosh^2(A) , \qquad (6.19)$$

in which (6.14) has been substituted. In (6.19) $V = 4\pi R^3 / 3$ is the volume of sphere with zero field pressure and A value has been defined in (6.12). By substitution of variables in (6.19) the integration can be reduced to the calculation of ψ - function values, where $\Psi(z) = \Gamma'(z)/\Gamma(z)$ – the derivative of gamma-function logarithm. There we taking into account the existence of following integrals [8]:

$$\beta(z) = \int_0^1 \frac{t^{z-1} dt}{1+t} ,$$

$$I(\mu) = \int_0^\infty \frac{exp(\pm \mu t) dt}{cosh^2 t} = \mp \mu \beta(\mp \mu / 2) - 1 ,$$

$$\beta(z) = \frac{1}{2}\left[\psi\left(\frac{z+1}{2}\right) - \psi\left(\frac{z}{2}\right)\right].$$

Not to violate the convergence of $I(\mu)$ integral, $-2 < \mu < 2$ condition with $\mu = (1+\alpha^2)^{-1/2} > 0$ must be executed. This condition is executed for the whole region of change of $3 \le \alpha < \infty$ parameter. Then the number of particles (6.19) can be estimated from following relation

$$N_1 = \frac{N_*}{2\alpha^2} exp(\mu d)[\Psi(1/2 + \mu/4) - \Psi(\mu/4) - \Psi(1/2 - \mu/4) + \Psi(1 - \mu/4)] , \qquad (6.20)$$

where $N_* = 3n_0 V$ – the scale of particles' number, $d = Arcosh\left(\sqrt{1+\alpha^2}/\alpha\right)$.The recurrent formula $\Psi(z+1) = \Psi(z) + 1/z$ has been exploited for reception of (6.20). We shall transform (6.20) to the form

$$N_1 = \frac{N_*}{2\alpha^2} exp(\mu d)[\psi(3/2 + \mu/4) + \psi(2 - \mu/4) -$$

$$-\psi(1 + \mu/4) - \psi(3/2 - \mu/4) + \frac{8\mu}{4-\mu^2} + \frac{8(2-\mu)}{\mu(4-\mu)}] . \qquad (6.21)$$

In (6.21) the table values of Ψ - function, assigned in the interval from 1 to 2, can be used (see [8]). As it is seen from (6.21), at $\alpha \to \infty$ the reduced number of particles, being confined by the field, decreases by $\frac{N_1}{N_*} \sim \frac{2}{\alpha}$ law.

The additive mass of the cluster can be easy estimated from

$$M_1 = mN_1 = M_0 f(\alpha), \tag{6.22}$$

where $M_0 = mN_*$ – the scale of mass of the first kind traps.

8. The Results of Numerical Simulation

The numerical simulation of equation (6.1) (details are in [6]) has been executed for $\varphi(R) = \varphi_0 = 0,\ \varphi'(R) = 0$ field initial conditions with the step 10^{-4}. The special formulas of the Runge-Kutta method with 4-order's accuracy have been chosen to do it [9]. During simulation an equal-zero condition of the sum (4.4) of field's pressure and particles' pressure gradients has been executed automatically. Here, under radial dependence, this condition is reduced to the equation (6.1).

Figure 2 shows the radial distributions of normalized particle number density n/n_0 of spherical cluster for the various parameters of state. The curve 1 has been calculated for the value α=0.5; the curve 2 – for α=0.7; the curve 3 – for α=1.0; the curve 4 – for α=3.0. From figure 2 one can see the way of filling the cluster by particles under the change of cluster's temperature in the vicinity of temperature scale value $T \sim T_*$. The curve 4 shows the existence of hollow inside the cluster, and curves 1, 2, 3 point out the fact that when the temperature grows, the whole volume of cluster has been filled by the particles completely. The distribution function of particles' number density in the center of cluster tends to zero for all curves.

The details of numerical simulation of radial distributions of major physical parameters of hollow clusters one can find in [6].

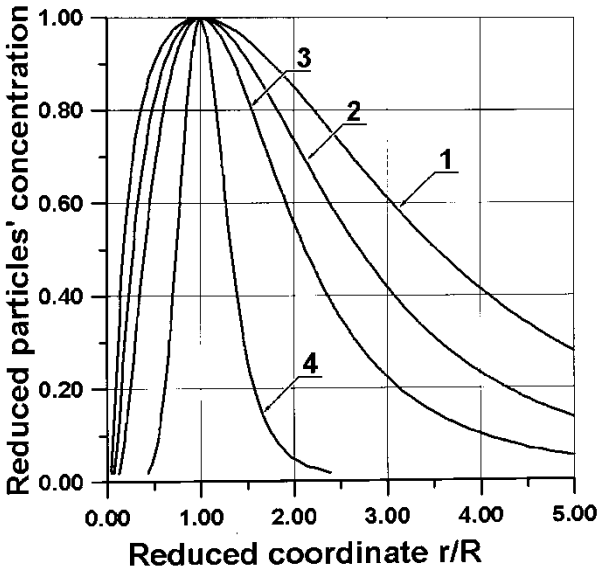

Figure 2: The Number Density Distribution of Particles in the Field Trap of First Kind

The external border r_2/R of the cluster and normalized values of the hollow r_1/R have been submitted in comparison table 1. These values have been defined via approximate solutions and numerical simulation out of $n_{1,2} = 0{,}01 n_0$ condition.

A	3	4	5	6	7	8	9	10
r_1/R	0,284	0,411	0,503	0,572	0,624	0,665	0,699	0,726
r_2/R	2,244	1,891	1,692	1,564	1,476	1,412	1,362	1,323
N_1/N_*	0,812	0,561	0,431	0,351	0,297	0,257	0,227	0,204
r_1/R	0,399	0,494	0,564	0,618	0,660	0,694	0,722	0,746
r_2/R	2,689	2,123	1,831	1,656	1,541	1,460	1,400	1,353
N_1/N_*	1,220	0,640	0,463	0,368	0,307	0,264	0,232	0,207

Table 1: The Results of Numerical Simulation

The values of function $N_1 / N_* = f(\alpha)$ for the same values of state parameter α have been submitted in the table 1. Three lower rows contain the results of numerical simulation with $1 \cdot 10^{-3}$ accuracy and three rows above them – the results, being given by approximate solution with the same accuracy.

9. Spherical Field Trap of Second Kind

The exact solution (6.2), obtained by Frenkel [3], has a form

$$y(x) = -\log(\alpha x). \tag{7.1}$$

Coming back to the potential, we receive one-parametric law for $\varphi(r)$ distribution

$$\varphi = \varphi_0 + \varphi_* \log(r / l), \tag{7.2}$$

where l – the spatial scale (5.2), and φ_0 – the parameter of distribution.

As one can see from (7.2), potentials' difference and its equivalent potential energy of system $U = m(\varphi - \varphi_0)$ have two signs. They are negative for the substance in the region $r / l < 1$ and are positive – in the $r / l \geq 1$ region. The potential distribution has two singular points: $r = 0$, $r \to \infty$. The value of potential $\varphi = \varphi_0$ belongs to the sphere with $r = l$ radius. The potential energy has no familiar minimum, but it looks like infinitely deep logarithmic slot.

The basic gravity-static and kinetic characteristics of the second kind traps follow from (7.2). The projected radial component of the field strength has a form

$$g_r / g_0 = -l / r, \tag{7.3}$$

where $g_0 = \varphi_* / l$ coincides with the scale of field strength at the plane case. The strength of trap's self-consistent field has been always directed to the center of system and has the singularity of $\sim -r^{-1}$ type at zero.

The system has been unlimited in the space. The density, the number density and the pressure of particles have the distribution with singularity of $\sim r^{-2}$ type at zero

$$\rho / \rho_0 = n / n_0 = p / p_0 = l^2 / r^2. \tag{7.4}$$

As it is seen from (7.4), in traps of the second kind the field pushes out the particles into infinitely deep slot, formed by the potential energy of system in the origin of coordinates.

The substance of cluster has disappeared at infinitely large distance from the center of system only. It points out at the principle difference of the second kind states and the states, observed earlier. *In the field traps of the second kind the number density is decreasing function of increasing radius.*

The pressure of field has singularity of $\sim r^{-2}$ type at zero

$$D / D_0 = l^2 / r^2 , \tag{7.5}$$

where $D_0 = p_0 = g_0^2 /(8\pi\gamma)$ coincides with the scale of field pressure at the plane case.

The total pressure of system is already not the integral of equation, as it varies by the law

$$P = D + p = 2p_0 l^2 / r^2 \neq const . \tag{7.6}$$

The pressure gradient of particles has been always directed along the strength of system's self-consistent field and has singularity of $\sim -r^{-3}$ type at zero

$$dp / dr = -f_0 l^3 / r^3 , \tag{7.7}$$

where $f_0 = 2p_0 / l$ coincides with the scale of pressure gradient at the plane case.

The radial component of self-consistent field's pressure gradient (the Bernoulli compensating force) has been directed opposite to the strength and has a singularity of $\sim r^{-3}$ type at zero

$$G_r = 4D / r + dD / dr = f_0 l^3 / r^3 . \tag{7.8}$$

It is obvious from (7.7) and (7.8) that the condition of confinement of arbitrary elementary volume in the field trap of the second kind has been realized at all points, except the singular one, being tended to $r \to 0_+$:

$$G_r + dp / dr = 0 . \tag{7.9}$$

Due to this fact the system, occupying the infinity volume, can be limited artificially by choose of internal system's radius r_1 (radius of the hollow), inside which the substance is absent, and of external system's radius r_2, outside of which the substance is absent too.

Let us calculate from (7.4) the overall number of particles, being confined by hollow cluster

$$N_2 = \int_{r_1}^{r_2} n(r) 4\pi r^2 dr = 2kTd /(m^2\gamma) , \tag{7.10}$$

where $d = r_2 - r_1$ is the thickness of layer, occupied by particles. It is seen from (7.10), as gravitating particle's mass is less, so the number of particles, being confined by cluster's field, is more under the other equal conditions.

The additive mass of cluster is obtained from (7.10)

$$M_2 = mN_2 = 2kTd /(m\gamma) . \tag{7.11}$$

This mass increases with growing of temperature, layer's thickness and turns out to be as more as the mass of gravitating particle is less.

10. The Similarity Relation in the Field Traps

Let us investigate the similarity properties of the field traps, consisting from gravitating particles with identical masses, and express the spatial scale of length (5.2) in the form

$$l = C(T / n_0)^{1/2} , \tag{8.1}$$

where

$$C = m^{-1}(k / 2\pi\gamma)^{1/2} = const_1 . \tag{8.2}$$

Introduce the scale of mass of the field trap

$$M_* = 2kTl / m\gamma = FT^{3/2} n_0^{-1/2} , \tag{8.3}$$

where

$$F = m^{-2}(2/\pi)^{1/2}(k/\gamma)^{3/2} = const_2. \quad (8.4)$$

By exception of number density from (8.1) and (8.3), we come to the linear connection between the spatial scale and the scale of mass under given value of temperature:

$$l = EM_* / T, \quad (8.5)$$

where $E=C/F= m\gamma /(2k) =const_3$.

The next similarity relations are followed from (8.5):

a) relation of the scale of mass to the scale of length is the same for systems with identical temperature. So, the scale of mass is greater, the scale of length is greater too. The inverse is also true.

b) more hot object has the less spatial scale under identical scales of masses of objects. The inverse is also true.

c) objects with identical relation of the scale of mass to the temperature have the same spatial scale.

By exception of object's temperature from (8.1) and (8.3) we obtain, that the scale of object's mass is always proportional to the scale of its $n_0 l^3$ particles' number:

$$M_* = 4\pi m n_0 l^3. \quad (8.6)$$

Let's attract from (6.22) the value of the scale of mass M_0 in the field traps of first kind

$$M_0 = mN_* = 3n_0 mV = 4\pi R^3 m n_0, \quad (8.7)$$

determine the ratio of this scale to the scale of mass

$$M_0 / M_* = 2\pi R^3 m^2 n_0 \gamma /(kTl) = \alpha^3 \quad (8.8)$$

and write the trap's mass in account with (8.8)

$$M_1 / M_* = \alpha^3 N_1 / N_*. \quad (8.9)$$

It is seen from (8.9) that field traps with potential well have a large capacity. At the other identical conditions their masses can exceed the scale of mass on one or two orders under change of the state parameter in $3 \le \alpha \le 10$ range (see table 1).

Let's discriminate three types of states, in which the field trap of second kind can stay. The first state is the state with negative potential energy, i.e. $U = m(\varphi - \varphi_0) < 0$. In this state the field trap has $r_2 < l$ external radius. The radius of internal hollow r_1 one can find from the largest values of number density of particles, which are known in the nature and attainable in nucleus $n_1 \approx n_n \approx 10^{38}$ cm^{-3}.

Then the mass of such closely packed object can be submitted as

$$M_2 = M_*(\chi - \zeta), \quad (8.10)$$

where $\zeta = r_1 / l = \sqrt{n_0 / n_n}$ – normalized radius of the hollow and $\chi = r_2 / l = \sqrt{n_0 / n_2} < 1$ – normalized external radius. It is seen from (8.10) that the mass is $M_2 < M_*$ in such states.

The states with positive potential energy, having large hollow, are realized under $\zeta \ge 1$ condition. In such states under $\chi > 1 + \zeta$ the mass is $M_2 \ge M_*$ and under $0 < \chi < 1 + \zeta$ it is $M_2 \le M_*$ mass.

At the intermediate states the ratio of mass can be an arbitrarily value under execution of the following inequalities: $0 < \zeta < 1$, $\chi > 1$. In the presence of close packing ($\zeta \to 0$) at the intermediate states the mass of object will be large under $\chi >> 1$ condition:

$$M_2 = M_* \chi . \tag{8.11}$$

If the value of thickness of the layer, occupied by particles, is equal to the value of the spatial scale $d=l$, so the variable is $\chi = 1 + \zeta$ and it is $M_2 = M_*$ mass.

11. Parameters of the Field Traps, Consisting of Neutrons with High Temperature

For the field trap, holding neutrons, the values of permanent coefficients are following: C=1,0837·10^{19} $(cm\ K)^{-1/2}$; F=2,6785·10^{34} $g\ (cm\ K)^{-3/2}$; E=4,0459·10^{-16} $cm\ K\ g^{-1}$. It is followed from (8.5) that for neutrons, being under the temperature T=10^{12} K, while the scale of mass M_* is changed from 2·10^{39} till 2·10^{42} g, the spatial scale l is changed in the limits of 8·10^{11} to 8·10^{14} cm. The inequalities limit the interval of possible changes of value n_0 in the range from 1,8·10^{20} till 1,8·10^{26} cm^{-3}. They are far from n_n - the average nuclear number density of the substance. The estimates, obtained from relations of similarity, permit to execute the correct calculations.

At the table 2 the dependences of the scales of the field traps from n_0 have been adduced in assumption that they consist of neutrons, heated to the temperature T=10^{11} K (i.e., on one order more than in neutrons stars [10]), and the value n_0 can changes in the range of 2,0·10^{20} to 2,0·10^{26} cm^{-3}.

$n_0(cm^{-3})$	$M_*(g)$	$l\ (cm)$
0,2·10^{21}	0,599·10^{41}	0,242·10^{15}
0,2·10^{22}	0,189·10^{41}	0,766·10^{14}
0,2·10^{23}	0,599·10^{40}	0,242·10^{14}
0,2·10^{24}	0,189·10^{40}	0,766·10^{13}
0,2·10^{25}	0,599·10^{39}	0,242·10^{13}
0,2·10^{26}	0,189·10^{39}	0,766·10^{12}
0,2·10^{27}	0,599·10^{38}	0,242·10^{12}

Table 2: The Dependence of Scale of Mass and Spatial Scale from Number Density

At the table 3 the results of numerical simulation of super-massive clusters' parameters for the field traps of first and second kinds, being under the same conditions as in the table 2, are placed. The next algorithm of simulation has been accepted. One must:

1. Calculate the spatial scale (5.2) by given n_0 and T.
2. Determine radius R of the sphere of zero field pressure for given α from the formula (6.3).
3. Break down the distribution of number density in the points with $n_{1,2} = 0{,}01 n_0$ and find normalized values of the hollow's radius r_1/R and external border's radius r_2/R, depending on the state parameter α (see the second and the third row from the bottom of the table 1 for the field traps of first kind).
4. Calculate the scale of $N_* = 4\pi R^3 n_0$ particles' number.
5. Find the values of normalized number of particles $N_1(3)/N_* = 1{,}220$ under α=3 and $N_1(10)/N_* = 0{,}207$ under α=10

from the table 1 (the lower row).

6. Calculate the additive mass of the field trap of first kind from (6.22).

7. Assume that for the field trap of second kind the radius of the field trap's hollow coincides with r_1 and its external radius – with r_2.

8. Find the number of particles and the mass for the field trap of second kind from relations (7.10), (7.11).

The state parameter α=3						
n_0, cm^{-3}	r_1, cm	r_2, cm	N_1	N_2	M_1/M_s	M_2/M_s
$0{,}2\cdot10^{21}$	$0{,}290\cdot10^{15}$	$0{,}195\cdot10^{16}$	$0{,}118\cdot10^{67}$	$0{,}246\cdot10^{66}$	$0{,}991\cdot10^{9}$	$0{,}207\cdot10^{9}$
$0{,}2\cdot10^{22}$	$0{,}918\cdot10^{14}$	$0{,}618\cdot10^{15}$	$0{,}373\cdot10^{66}$	$0{,}777\cdot10^{65}$	$0{,}314\cdot10^{9}$	$0{,}654\cdot10^{8}$
$0{,}2\cdot10^{23}$	$0{,}290\cdot10^{14}$	$0{,}195\cdot10^{15}$	$0{,}118\cdot10^{66}$	$0{,}246\cdot10^{65}$	$0{,}991\cdot10^{8}$	$0{,}207\cdot10^{8}$
$0{,}2\cdot10^{24}$	$0{,}918\cdot10^{13}$	$0{,}618\cdot10^{14}$	$0{,}373\cdot10^{65}$	$0{,}777\cdot10^{64}$	$0{,}314\cdot10^{8}$	$0{,}654\cdot10^{7}$
$0{,}2\cdot10^{25}$	$0{,}290\cdot10^{13}$	$0{,}195\cdot10^{14}$	$0{,}118\cdot10^{65}$	$0{,}246\cdot10^{64}$	$0{,}991\cdot10^{7}$	$0{,}207\cdot10^{7}$
$0{,}2\cdot10^{26}$	$0{,}918\cdot10^{12}$	$0{,}618\cdot10^{13}$	$0{,}373\cdot10^{64}$	$0{,}777\cdot10^{63}$	$0{,}314\cdot10^{7}$	$0{,}654\cdot10^{6}$
$0{,}2\cdot10^{27}$	$0{,}290\cdot10^{12}$	$0{,}195\cdot10^{13}$	$0{,}118\cdot10^{64}$	$0{,}246\cdot10^{63}$	$0{,}991\cdot10^{6}$	$0{,}207\cdot10^{6}$
The state parameter α=10						
n_0, cm^{-3}	r_1, cm	r_2, cm	N_1	N_2	M_1/M_s	M_2/M_s
$0{,}2\cdot10^{21}$	$0{,}181\cdot10^{16}$	$0{,}328\cdot10^{16}$	$0{,}740\cdot10^{67}$	$0{,}217\cdot10^{66}$	$0{,}623\cdot10^{10}$	$0{,}183\cdot10^{9}$
$0{,}2\cdot10^{22}$	$0{,}571\cdot10^{15}$	$0{,}104\cdot10^{16}$	$0{,}234\cdot10^{67}$	$0{,}687\cdot10^{65}$	$0{,}197\cdot10^{10}$	$0{,}578\cdot10^{8}$
$0{,}2\cdot10^{23}$	$0{,}181\cdot10^{15}$	$0{,}328\cdot10^{15}$	$0{,}740\cdot10^{66}$	$0{,}217\cdot10^{65}$	$0{,}623\cdot10^{9}$	$0{,}183\cdot10^{8}$
$0{,}2\cdot10^{24}$	$0{,}571\cdot10^{14}$	$0{,}104\cdot10^{15}$	$0{,}234\cdot10^{66}$	$0{,}687\cdot10^{64}$	$0{,}197\cdot10^{9}$	$0{,}578\cdot10^{7}$
$0{,}2\cdot10^{25}$	$0{,}181\cdot10^{14}$	$0{,}328\cdot10^{14}$	$0{,}740\cdot10^{65}$	$0{,}217\cdot10^{64}$	$0{,}623\cdot10^{8}$	$0{,}183\cdot10^{7}$
$0{,}2\cdot10^{26}$	$0{,}571\cdot10^{13}$	$0{,}104\cdot10^{14}$	$0{,}234\cdot10^{65}$	$0{,}687\cdot10^{63}$	$0{,}197\cdot10^{8}$	$0{,}578\cdot10^{6}$
$0{,}2\cdot10^{27}$	$0{,}181\cdot10^{13}$	$0{,}328\cdot10^{13}$	$0{,}740\cdot10^{64}$	$0{,}217\cdot10^{63}$	$0{,}623\cdot10^{7}$	$0{,}183\cdot10^{6}$

Table 3: The Results of Numerical Simulation of Super-Massive Clusters' Parameters for the Traps of First and Second Kinds

We record into the first column of the table 3 the value of n_0, to the second one – the radius of hollow, to the third column – the external radius of cluster, to the fourth one – the number of particles in the trap of first kind, to the fifth – the number of particles in the trap of second kind, in the six column – the mass of cluster in the trap of first kind, related to the mass M_s of the Sun, to the seven - the mass of cluster in the trap of second kind, related to the mass M_s of the Sun too.

It is seen from the table 3, that the mass of the field trap of first kind is more than the mass of the field trap of second kind under the same parameters. This distinction increases with α growth. The relation (8.9) explains the reason of it. The mass of the field trap of first kind increases with the growth of state parameter α. The increase of the number density n_0 leads to the decrease of the trap's mass and of external radius of the cluster (see 8.5) under the permanent α. The inverse is also true.

The simulation shows that the growth of cluster's temperature on the order (for identical state parameters) leads to the growth of mass of the field traps of second kind more than an order. At the same time the range of their masses exceeds the range of masses of the field traps of first kind under original temperature with negligible changing of external radius of the cluster.

The external dimensions of clusters under the lower values n_0 exceed the mean radius of Solar system from 10-th to 18-th times only. The value of greater semi-axis of Pluto's orbit ~ $0{,}6\cdot10^{15}$ *cm* [see 11] has been taken as the mean radius of Solar system.

Since it has been appeared in accepted algorithm, that ζ value is $\zeta = r_1 / l > 1$, so only masses of the field traps of second kind with positive potential energy have entered into the table 3. Under the temperature $T=10^{11}$ K and at the close packing in intermediate states, the radius of the hollow is $r_1=3{,}42\cdot10^5$ *cm* and the parameter is $\zeta=1{,}41\cdot10^{-6}<<1$ at the upper value of n_0. Then masses of the field traps of second kind get into $10^6 M_s < M_2 < 10^9 M_s$ range. They have the external radius r_2, which value gets into the range from $8\cdot10^{12}$ till $8\cdot10^{15}$ *cm*. Under identical conditions the parameter is $\zeta=1{,}41\cdot10^{-9}<<1$ at the lower value of n_0, but the value of radius r_2 gets into the same range as above.

In conclusion, for the state parameter $\alpha=3$ and $n_0=0.2\cdot10^{21}$ cm^{-3}, we present the scales of physical quantities, describing the equilibrium state of the neutron cluster: temperature's scale $T_*=9.0\cdot10^{11}$ *K*; potential's scale $\varphi_*=1.65\cdot10^{19}$ $(cm/s)^2$; intensity's scale $g_*=2.27\cdot10^4$ cm/s^2; maximum pressure at the bottom of the well $p_0=2.76\cdot10^{15}$ $dyne/cm^2$; field's pressure scale $D_*=3.07\cdot10^{14}$ $dyne/cm^2$; gradient's pressure scale $f_*=22.7$ $dyne/cm^3$. An increase in the value of n_0 on six orders of magnitude leads to increase in the intensity's scale on three orders of magnitude, the pressure's scale on six orders of magnitude, and the pressure gradient's scale on nine orders of magnitude.

The wall of the field traps of first kind can contain a set of layers with varying density. In a trap with mass of 10^9 M_s relative to zero-pressure sphere, a set of symmetric layers is realized: a super-dense layer with $\rho\sim10^5$ g/cm^3; a layer with metal density of $\rho\sim10^4$ g/cm^3; a liquid layer with $\rho\sim10^3$ g/cm^3; a gas layer $\rho<10^2$ g/cm^3. A trap with mass of 10^6 M_s consists of inhomogeneous gas.

The wall of the field traps of second kind with large mass can also contain a set of layers. The densest layer will start from the surface of the hollow r_1. The inhomogeneous gas will be adjacent to the external radius of the trap r_2.

The formation of layers with different densities occurs during the process of clustering of matter. The process is responsible for the formation of solid matter in space. It occurs when the compression forces of the layer begin to prevail over the expansion forces, and collapse occurs. This process is universal. It can occur in a thundercloud with dense atmospheric gas. Clustering leads to the appearance of numerous liquid droplets, which, under strong compression, are accompanied by the formation of hail. It should be noted that the sizes of the bubbles of mass particles differ greatly. In the case of space, compression is arisen due to gravitational forces, and in the case of liquid droplets, by the strength of the collective electric field. These forces differ between themselves by a factor of 10^{23}.

Note that from relation (7.11) we can obtain the observed value of average temperature of the Sun. It can be under the assumption that a uniformly heated sphere is completely filled with liquid plasma at $d=R$. The temperature has a value of $1.1\cdot10^7$ K and coincides with estimate in the Chandrasekhar model [2] with fine-resolution.

12. Invisible Bubbles from the Sun's Dark Plasma

Canonical physics of mass particles' interaction predicts the existence of low-temperature plasma clusters of small radii with large masses. They can be identified with heavy invisible thin-walled bubbles. From (7.11) it follows that with a radius of ~ $140\cdot10^5$ *cm* and a temperature of 1 *K*, with a liquid wall thickness of 0.1 *cm*, they have a mass of ~ $2.5\cdot10^{14}$ *g*.

Where can such cold bubbles arise? Oddly enough, they can arise in near-solar space. They are generated by the dark plasma of the Sun. You can find NASA videos in the Internet. There, heated plasma ejected by the Sun turns into dark plasma. During this transition, the heated plasma contains balls with hot plasma. They are ejected from the surface of the Sun in the direction of the solar wind and at its speed. Let us estimate their mass spectrum for radii from 3 *cm* to 10^7 *cm* (see Table 4) at an average density of liquid solar plasma of 1.4 g/cm^3[11].

R	3 cm	1 m	100 m	1 км	100 км
M (кг)	0,16	$5{,}9\cdot10^3$	$5{,}9\cdot10^9$	$5{,}9\cdot10^{12}$	$5{,}9\cdot10^{18}$

Table 4: Masses of Balls Completely Filled With Liquid Plasma

The values of the masses of balls containing liquid plasma should be reduced from six to nine orders of magnitude. The reason is that balls fly out from the surface of the Sun, the temperature of which is thousands of times lower than inside the Sun, and as they move they are stripped by plasma of solar corona. Flying out into vacuum, filled balls turn into thin-walled bubbles with a liquid wall (density 1 g/cm^3) due to expansion of the bubble and its cooling. The cooling to a temperature, lower than the excitation temperature of hydrogen atom $1.2\cdot10^5$ *K* (for a neutron it is on 2-3 orders of magnitude higher), transfers these bubbles to the class of non-radiating matter. They become invisible. Thus, a new class of matter is formed, consisting of known substance - dark matter of near-solar space.

Invisible bubbles of hydrogen or helium can have diameters from 100 cm to 10^7 cm. To be bear from dark plasma of the Sun, they have already been recently registered in near-Earth space, near the Moon's surface and on the Earth. When falling down to the Earth, bubbles fly through the atmosphere. Their temperature can increase on one to two orders of magnitude, and the radii of bubbles can decrease on one to two orders of magnitude too. Their traces were noticed in Russia in the fields of fallen wheat by «Kosmopoisk» group (2019, circles of V. Chernobrov [12]).

They can be responsible to depressurization of spacecraft, to inelastic impacts on the station's windows, and even to recent unsuccessful landings of spacecraft on the Moon. Trajectory's measurements of lunar landing may contain information about physical parameters of invisible bubbles that changed their landing speed. Processing of measurements can give two independent experimental confirmations of the existence of previously unknown physical objects of heated mass particles - invisible bubbles. The confirmation of hypothesis of the existence of objects can lead to a world-class discovery. It will raise the prestige of research in the physics of cluster's state of the matter from heated mass particles in space.

The "damaging" factor of bubble's action should be considered its momentum. The average speed of solar wind is ~ 10^5 cm/s. With a bubble radius of $140\cdot10^5$ cm (temperature 1 K), a liquid wall thickness of 0.1 cm, its mass reduced by 10^6 times is ~ 250 tons, and reduced on another three orders of magnitude is 250 kg. The invisible bubble has a in the range from $2.5\cdot10^8$ kgm/s to $2.5\cdot10^5$ kgm/s. A train, consisting of 20 carriages by 60 tons' weigh of each and traveling with the speed from 210 m/s to 0.2 m/s, has the same momentum.

The soft collision of such bubble with the spacecraft or station can end the mission of the last ingloriously. The collision can shift it from intended trajectory and change the speed. Besides, there may be not any mechanical damage to devices. We are sure that invisible "solar artillery" may also be responsible to observed losses of communication satellites. The probability of successful flight of the spacecraft in near-Earth or near-Moon space in current time turns out to be greatly exaggerated. Apparently, we need to think about creating of motion's security service for spacecraft in near-solar space, which shall monitor space flights during "solar thunderstorm".

Heated gas bubbles with thin wall and radius close to 100 km or more could have left their mark on the Moon's surface. They formed a typical class of craters, which have a ridge of matter, melted in the form of a ring, and a smooth surface texture inside the ridge (see Fig. 3). A similar crater structure on metal was first discovered by K. Shoulders in 1980. It arose when micron-sized heated bubble of charges hit flat titanium surface and registered the existence of new physical object - a cluster of charges of the same sign [13].

13. Conclusion

The Tunguska phenomenon could have been a hollow, loose cosmic "snowball" of enormous mass, consisting of ice dust particles of nanoscopic dimensions (details in [14]). It was ejected by ice geysers from the depths of the Enceladus – the sixty-first satellite of the Saturn. The particle flow density of such ice "bubble", falling to the ground, will be significantly lower in the center than in the neighboring layers. This is indicated by solution to the problem of bubble, falling on a flat surface, found in [14]. Then, at the epicenter of the fall, produced destruction will be minimal and coincides with observations of the Kulik expedition. The memory of the fall of cosmic "snowball" is still preserved by the mast forest, not felled, remaining at the epicenter of the fall.

Figure 3: Traces of the fall of Heated Solar Bubbles with Thin Walls onto the Surface of the Moon, Similar to the Shoulders Crater

Acknowledgments

The authors express their gratitude to the academicians of the Russian Academy of Sciences: A.A. Krasovsky, B.I. Katorgin, V.A. Babeshko and the academician of the National Academy of Sciences of Ukraine V.G. Baryakhtar for their genuine long-term interest and moral support in the development of new scientific school: "Canonical Physics of Cluster States of Matter".

We are grateful to academicians of the Russian Academy of Natural Sciences: Professor L.G. Sapogin and pilot-cosmonaut V.A. Dzhanibekov, - for many years' fruitful discussion of results, being obtained in the work.

We would like to acknowledge the great assistance of L.K. Sapogina, who carried out the editing of Russian and English texts for our articles, brochures and monographs.

References

1. Emden, R. (1907). *Gaskugeln: Anwendungen der mechanischen Wärmetheorie auf kosmologische und meteorologische Probleme.* BG Teubner.
2. Chandrasekhar, S. (1950). Introduction to the Doctrine of Stellar Structure. Moscow: IL Publishing House.
3. Frenkel, Ya. I. (1948). Statistical Physics. Moscow-Leningrad: USSR Academy of Sciences Publishing House.
4. Kamke, E. (1976). Handbook of ordinary differential equations. *Chelsea Publ.*
5. Sapogin, V. G. (1996). Flat Self-Consistent Hamiltonian Systems of Gravitating particles//Proceedings of the Higher Educational Institutions of the North Caucasus Region. Series: Natural Sciences. No. 3. pp. 72-79.
6. Sapogin, V. G. (2000). Mechanisms of Matter Confinement by a Self-Consistent Field. Taganrog: TRTU Publishing House.
7. Sapogin, V. G. (2003). On a Class of Exact Solutions to the Emden Equation. Proceedings of the Higher. Educational. Head of the North Caucasus Region. Series: Natural Sciences. No. 3. P. 55-56.
8. Prudnikov, A. P., Brychkov, I. A., & Marichev, O. I. (1981). Integraly i riady: elementarnye funktsii. Nauka.
9. Korn, G., & Korn, T. (1974). Handbook of Mathematics for scientists and engineers.
10. Dyson, F., Ter Haar, D., Bondarev, A. P., & Stanyukovich, K. P. (1973). Neutron stars and pulsars. *Neutron stars and pulsars*.
11. Pikelner, S. B. (1978). Little Encyclopedia. Physics of Space. M., p. 655.
12. Chernobrov, V. (2019). Crop Circles in Russia and the USSR. ONIO "Kosmopoisk", p. 72.
13. Shoulders, K. (1996). EV: A Tale of Discovery. 1987, Jupiter Technology, Austin TX; Shoulders Ken and Shoulders Steve, "Observation on the Role of Charge Clusters in Nuclear Cluster Reaction". *Journal of New Energy, 1*(3), 111-121.
14. Sapogin, V. G. (2009). Emden Gas Balls in a Self-Consistent Theory of Gravity. Taganrog: Publishing House of TI SFedU, – p. 99.